Interference Modeling in CSMA Multi-Hop Wireless Networks

Anthony Busson, Guillaume Chelius, Jean-Marie Gorce

INSTITUT NATIONAL DE RECHERCHE EN INFORMATIQUE ET EN AUTOMATIQUE

Interference Modeling in CSMA Multi-Hop Wireless Networks

Anthony Busson — Guillaume Chelius — Jean-Marie Gorce

N° 6624

Septembre 2008

Thème COM

ISSN 0249-6399 ISRN INRIA/RR--6624--FR+ENG

INSTITUT NATIONAL
DE RECHERCHE
EN INFORMATIQUE
ET EN AUTOMATIQUE

INRIA

centre de recherche
GRENOBLE - RHÔNE-ALPES

Interference Modeling in CSMA Multi-Hop Wireless Networks

Anthony Busson* , Guillaume Chelius† , Jean-Marie Gorce‡

Thème COM — Systèmes communicants
Équipes-Projets Ares

Rapport de recherche n° 6624 — Septembre 2008 — 20 pages

Abstract: In analytical studies of multi-hop wireless networks, the spatial distribution of transmitters is typically modeled using a homogeneous Poisson point process. In this article, we show how such a modeling is inaccurate and leads to an inappropriate interference distribution for CSMA/CA networks. We then study a more realistic model, the Matèrn point process, which still reveals some unexpected flaws such as an under-estimation of the transmitters density. To get round these limitations, we propose the use of an alternate model, referred to as *Simple Sequential Inhibition* (SSI) point process, which we assert being a valuable and more appropriate model for CSMA/CA networks. We present some analytical results on the Matèrn and SSI models and we conjecture and show by simulation that, with both models, the interference distribution converges towards a Normal distribution.

Key-words: interference modeling, stochastic geometry, multi-hop wireless networks, SSI point process, Matèrn point process

* IEF - CNRS, 91405 Orsay, France - anthony.busson@u-psud.fr
† INRIA, University of Lyon, INSA-Lyon, CITI, F-69621, France - guillaume.chelius@inria.fr
‡ University of Lyon, INRIA, INSA-Lyon, CITI, F-69621, France - jean-marie.gorce@insa-lyon.fr

Centre de recherche INRIA Grenoble – Rhône-Alpes
655, avenue de l'Europe, 38334 Montbonnot Saint Ismier
Téléphone : +33 4 76 61 52 00 — Télécopie +33 4 76 61 52 52

Modelisation des interférences dans les réseaux sans-fil multi-sauts

Résumé : Dans les études analytiques concernant les réseaux sans-fil multi-sauts, la distribution spatiale des émetteurs est généralement modélisée par un processus ponctuel de Poisson. Dans cet article, nous décrivons les limites de ce modèle et leurs conséquences sur la distribution du niveau d'interférence dans des réseaux de type CSMA/CA. Nous étudions ensuite un modèle plus réaliste, le processus ponctuel de Matèrn, qui présente également un certains nombres de défauts conduisant à une sous-évaluation du nombre d'interférants. Afin de contourner ces limitations, nous proposons finalement l'utilisation d'un troisième modèle, appelé processus ponctuel SSI (*Simple Sequential Inhibition*), que nous affirmons être d'avantage approprié dans le contexte des réseaux CSMA/CA. Nous présentons quelques résultats analytiques liés aux modèles SSI et Matèrn et après une étude par simulation, nous conjecturons que pour ces deux modèles, la distribution du niveau d'interférence converge vers une loi normale.

Mots-clés : modélisation des interférences, géométrie stochastique, réseaux sans-fil multi-sauts, processus ponctuel SSI, processus ponctuel Matèrn

1 Introduction

Multi-hop radio networks have been widely studied for more than 10 years. Some fundamental results have been obtained concerning the capacity and the connectivity of the network [9, 8] but at the price of strong assumptions about the physical layer. More recent works then addressed the performance evaluation of multi-hop radio networks under more realistic constraints. A first trend consists in improving the realism of the radio channel, including effects such as radiation patterns, fading and shadowing. As a deterministic study would require the knowledge of a specific environment, it appeared often more relevant to consider these phenomena from a statistical point of view [3, 11, 16, 17].

Taking into account interference is a second aim for improving the realism of multi-hop networks modeling. Several works introduced interference [11, 22] by modeling the overall interference power as a statistical variable including the contribution of all simultaneous transmitters. In most of these approaches, the lack of knowledge about the transmitter positions let authors considering the spatial distribution of the transmitters as Poisson distributed. This means that their positions are not correlated. Under complementary assumptions about the fading strength, this approach also lead to an analytical expression of the interference distribution [2].

In this paper, we first propose in section 3 to extend these results in a more general framework, *i.e.* for any fading and shadowing strengths, but from a numerical resolution only. We then point out the main limitations of this model. Indeed, most of wireless networks exploit a resource sharing technology, which means that the existence of two interferers in their vicinity is not possible. Concerning CSMA/CA-like networks, it has been earlier proposed that using a Matèrn point process [2] may lead to a more realistic model as it allows to introducing an exclusion area around nodes. Albeit, we show in Section 4 that this model suffers from some unexpected properties, such as an underestimation of concomitant active transmitters. Further, this model cannot model the cumulative level of several interferers. To get round these limitations, we propose in section 5 the use of an alternate model, referred to as *Simple Sequential Inhibition* (SSI) point process, which we assert being a valuable and more appropriate model for CSMA/CA networks. In Section 6, we present some analytical results on the Matèrn and SSI models and we conjecture and show by simulation that, with both models, the interference distribution converge towards a Normal distribution. We finally conclude in Section 7.

2 Physical layer modeling

2.1 Propagation modeling

At a given location x_j ($x_j \in I\!R^2$), the power of a signal received from node x_i is given by $S_i \cdot h_{ij}$ where h_{ij} is the path-loss over (x_i, x_j) , and S_i the transmission power of x_i. The path-loss function depends on the propagation model. In most cases, one have $h_{ij} = l(\|x_j - x_i\|)$ where $\|.\|$ is the Euclidean norm in $I\!R^2$ and $l(.)$ is a decreasing function from $I\!R^+$ in $I\!R^+$, standing for the power decay with respect to the distance. In the simplest scenario, *i.e.* in line of sight (LOS), the path-loss is classically modeled using a power-law function derived from the Friis formula [20]: $l(u) = A_0 \cdot u^{-\alpha}$ where A_0 is a constant related to physical parameters and β is a parametric path-loss exponent typically ranging from 2.0 to 6.0.

Basically, the Friis formula has been derived for far field conditions and is not further valid in the vicinity of the receiver. Thus, a more realistic model can be obtained by bounding this function near 0. In the following, when not otherwise stated, our results are valid for any bounded continuous decreasing function $l(.)$ and numerical simulations are obtained having $l(u) = min(1, u^{-\alpha})$ with $\alpha > 2$.

In urban and indoor environments, more complicated scenario occur due to *shadowing* and multi-paths, *i.e. fading*. These phenomena are statistically modeled through the introduction of two stochastic variables, $\mathbf{s}_{ij}$ and $\mathbf{f}_{ij}$: $\mathbf{h}_{ij}(t) = l(\|x_j - x_i\|) \cdot \mathbf{s}_{ij} \cdot \mathbf{f}_{ij}(t)$. $\mathbf{s}_{ij}$ is defined as a correlated spatial stochastic process but roughly constant with respect to time. The most usual shadowing model is the logNormal shadowing. On the opposite, fading $\mathbf{f}_{ij}$ which stands for small scale phenomenon due to the incoherent summation of multiple paths, can be considered as a spatially non correlated ant time variant process. Usual models for $\mathbf{f}_{ij}$ are the exponential distribution for *Rayleigh fading* and a Gamma distribution for *Nakagami fading* [20].

2.2 Interference modeling

As mentioned before, interference plays a fundamental role in the capacity of wireless networks. When a single channel is used for several nodes, interference is referred to as co-channel interference. It is usual to considere the overall interference as a corruptive noise which affects the reception quality. In this case, the interference strength is equal to the sum of the interfering signals:

$$\begin{aligned} I_\Phi(x_j, t) &= \sum_{x_i \in \Phi} S_i \cdot h_{ij}(t) \\ &= \sum_{x_i \in \Phi} S_i \cdot l(\|x_j - x_i\|) \cdot \mathbf{s}_{ij} \cdot \mathbf{f}_{ij}(t) \end{aligned} \quad (1)$$

where Φ is the set of interfering nodes.

The use of this equation is valid only for linear receivers and only if the interference behaves roughly like the receiver noise. This assumption may fail if the number of interferers is low or if it exists one or few interferers having a higher power than the others. In this case, these strong interferers produce a correlated noise which affects in depth the performance of the receiver. In many applications, this problem doesn't hold because a medium access control (MAC) policy is used to prevent nearest interferers.

3 Modeling of non CSMA/CA networks

In analytical studies of multi-hop wireless networks [2, 5, 6], the location of emitters is typically modeled using a homogeneous Poisson point process Φ.

3.1 Interference Probability Density Function

In most of analytical evaluations [2, 1], S_i and $\mathbf{s}_{ij}$ are supposed constant whereas $\mathbf{f}_{ij}(t)$ is supposed independently and exponentially distributed. Thanks to these assumptions, closed formulae were obained [1, 2] but their validity is limited to a particular radio environment, that is with Rayleigh fading and no shadowing. To broaden this study to other distributions, we study the probability density function - *PDF* - of the interference I_Φ by the inversion of its Laplace transform. The probability density function can be

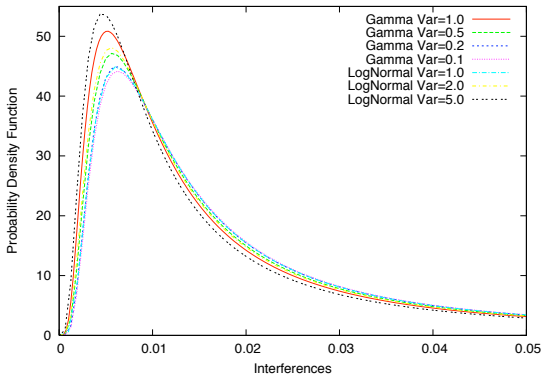

Figure 1: Interference Probability Density Function in the Poisson model.

numerically evaluated for any distribution of S_i, $\mathbf{s}_{ij}$ and $\mathbf{f}_{ij}$ under the condition that I_Φ remains almost surely finite. Thus, we numerically extend the results of [1] with the computation of a frame reception probability in general radio models.

Figure 3.1 depicts the *PDF* of interference with logNormal shadowing and Nakagami fading, for varying variances of $\mathbf{s}_{ij}$ and $\mathbf{f}_{ij}$. For all parameters, the distribution presents a peak and a heavy-tail. This heavy-tail is not negligible as it has an important impact on the mean interference value ($\mathbb{E}[I_\Phi(x_j)] = 0.0471$). The distributions are thus strongly asymmetric and far from being Gaussian. This observation confirms the results of [26, 13, 7], where an heavy-tailed interference distribution has been observed for a Poisson distribution of interferers.

This observation is in contradiction with the assumption that is classically made in the signal processing community where the interference is generally considered to be Gaussian [25]. Several distributions such as K-distribution, Weilbull, logNormal or Laplacian distributions have been proposed to model or extrapolate these heavy-tailed distributions. More recently, the alpha-stable distributions have been also proposed [13].

3.2 Limitation to non CSMA/CA networks

With a Poisson point process, the transmitters' locations are assumed independent. This strong assumption is not valid in most of wireless multi-hop networks. The use of a *Medium Access Control* (MAC) protocol generally ensures that two close nodes do not emit simultaneously, either by assigning them different frequency (FDMA) or time (TDMA) resources or, for asynchronous systems, by implementing a CSMA/CA mechanism.

In a CSMA/CA network, a potential transmitter senses the channel before effectively transmitting. Depending on whether the channel is assessed clear or not, the transmission occurs or is postponed. *Clear Channel Assessment* (CCA) depends on the MAC protocol and the terminal settings. For the two most widely used CSMA/CA protocols, IEEE 802.11 DCF and IEEE 802.15.4, CCA is performed according to one of these three methods. (*mode 1*) CCA reports busy medium upon detecting any energy above the Energy Detection threshold. (*mode 2*) CCA shall report a busy medium only upon the detection of a compliant signal. (*mode 3*) CCA reports a busy medium using a *OR* or *AND* logical combination of the two previous conditions.

A direct consequence of CSMA/CA is that transmitters cannot be very closed to each others. The Poisson point process does not take into account this constraint and leads to a large inaccuracy in the distribution of emitters for a CSMA/CA network. This results in an inappropriate interference distribution as it will be shown in Section 6.

4 Modeling of CSMA-CA networks

An alternate point process has been evoked in [2] to model the location of transmitters in a CSMA/CA network and studied in [18] to model dense IEEE 802.11 networks: the Matèrn point process that was first introduced by Matèrn in [15]. A Matèrn point process is a particular thinning of a homogeneous Poisson point process Φ such that the distance between two selected nodes is always greater than r, $r > 0$. In our context, the Poisson point process represents the potential transmitters whereas the Matèrn point process models the effective ones.

To derive a Matèrn point process from Φ, a mark U_i, uniformly distributed in $[0, 1]$ is associated to each point of Φ. A point X_i is selected as a transmitter if and only if no node with a greater mark value is present in the ball centered at X_i and with radius r. The ball of radius r around a transmitter can be seen as an *exclusion* domain that prevents other nodes to transmit.

Thanks to its selection process, the Matèrn point process seems well-suited to model a network operating in CCA *mode 2* . Indeed, a transmitter postpones its emission upon detection of a compliant signal, *i.e.* the presence of a transmitter within detection distance, and not based on an interference level. However, temporal as well as spatial considerations reveals some fundamental limitations.

4.1 Temporal considerations

Extension of the Matèrn point process to other CCA modes is not trivial. In particular, considering an interference level instead of a distance during the selection process is not straightforward. The measure of the interference at a given point requires that a subset of transmitters has been already selected. Thus, it requires a temporal scheduling between the points.

One way to introduce a temporal dimension is to consider the point process in a finite area and to introduce the points sequentially in the observation window. We define a temporal Matèrn point process denoted $\Phi_M(n)$, by considering a sequence of random variables $(X_i)_{i=1,..,n}$ independently and uniformly distributed in a ball of radius R, denoted B. The point X_1 is distributed first and systematically selected in $\Phi_M(n)$. At the i^{th} step, the point X_i is distributed and selected in $\Phi_M(n)$ if and only if none of the previous points lies in B_{X_i}. The procedure stops when the n points have been considered. Note that if n follows a discrete Poisson law, we get the classical Matèrn restricted to B. The temporal sequence is equal to the mark sequence of the classical Matèrn. Section 4.3 presents some theoretical results on this temporal Matèrn point process.

4.2 Spatial considerations

The second flaw of the Matèrn point process relies on its selection process. A point of the point process Φ which has not been selected in the final Matèrn inhibits nevertheless all the other nodes with a lower marks within its exclusion ball. For instance, in

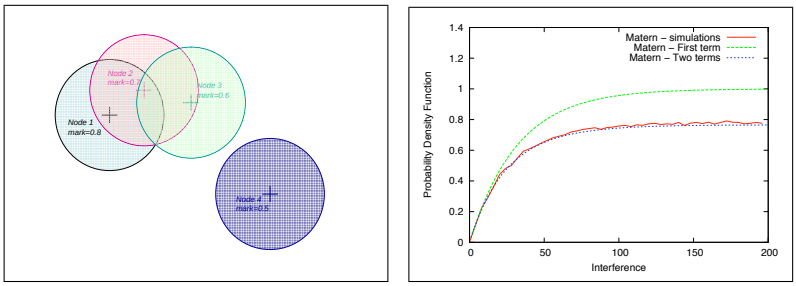

(a) An example of selection process. (b) *Packing density* w.r.t. n.

Figure 2: An example of selection process and packing density.

Figure 2(a), nodes 1 and 4 are selected as transmitters because they have the highest mark in their respective ball. Node 2 is not selected as it is within the ball of node 1. Node 3 is not selected as its mark is less to the one of node 2, despite the fact that node 2 is not selected. From the CSMA/CA perspective, this is inaccurate as only effective transmitters inhibit potential transmitters.

The fact that unselected points play a role in the selection process induces a partial coverage of the plane. Indeed, when the intensity of the underlying point process Φ tends to infinity, the union of the exclusion balls associated to the selected points covers only approximately 78% of the plane (see section 4.3). A large part of the transmitters which would be selected in reality is not considered in the Matèrn point process. The direct consequence is an underestimation of the effective transmitters intensity in the network and so far an underestimation of the interference level when compared to the reality.

4.3 Intensity, spatial distribution and coverage

We present here three results on the temporal Matèrn point process. The first one is simply the mean number of nodes in the observation area and its asymptotic behavior when R tends to infinity. A Proposition then gives the spatial distribution of k nodes randomly chosen among the points of $\Phi_M(n)$. The last Proposition presents a result on the mean coverage of the Matèrn.

Let $N_M(n)$ be the random variable describing the number of points in $\Phi_M(n) \cap B$, we get:

$$\begin{aligned}
\mathbb{E}\left[N_M(n)\right] &= \mathbb{E}\left[\sum_{i=1}^{n} \mathbb{1}_{X_i \in \Phi_M(n)}\right] = \sum_{i=1}^{n} \mathbb{P}\left(X_i \in \Phi_M(n)\right) \\
&= \sum_{i=1}^{n} \frac{(R-r)^2}{R^2}\left(1-\frac{\pi r^2}{\pi R^2}\right)^{i-1} + \int_{R-r}^{R} f(u)\left(\frac{A(u,r,R)-\pi r^2}{\pi R^2}\right)^{i-1} du \\
&= \frac{(R-r)^2}{R^2}\frac{R^2}{r^2}\left[1-\left(1-\frac{r^2}{R^2}\right)^{n}\right] + \int_{R-r}^{R} 2\pi u \frac{1-\left(\frac{A(u,r,R)-\pi r^2}{\pi R^2}\right)^{n}}{\pi R^2 - A(u,r,R) + \pi r^2} \quad (2)
\end{aligned}$$

where $A(u,r,R)$ denotes the area of the union of two discs of radius r and R with their centers at distance u.

$$A(u,r,R) = ur\sqrt{1-\left(\frac{1}{2}\frac{r^2+u^2-R^2}{ur}\right)^2} + u^2\arccos\left(-\frac{1}{2}\frac{r^2+u^2-R^2}{Rr}\right)$$

$$+R^2\arccos\left(-\frac{1}{2}\frac{r^2-u^2+R^2}{Rr}\right)$$

If $R \to +\infty$ and $n \sim \lambda\pi R^2$,

$$\lim_{R\to+\infty}\frac{\mathbb{E}\left[N_M(n)\right]}{\pi R^2} = \frac{1-e^{-\lambda\pi r^2}}{\pi r^2}$$

Proposition 1. *Let $\Phi_M(n)$ be a temporal Matèrn point process distributed in B, $(X_{i_1},..,X_{i_k})$ a subset of points of the original sequence $(X_i)_{i=1,..,n}$ with $1 \leq i_1 < i_2 < .. < i_k \leq n$, $kr^2 < R^2$ and $A_1,..,A_n$ a set of Borel set of $\mathbb{R}^2$ such that $A_i \subset B$ $\forall i = 1,..,k$, we get*

$$\mathbb{P}\left(X_{i_j} \in A_j \forall j \in \{1,..,k\}, X_{i_j} \in \Phi_M(n) \forall j \in \{1,..,k\}\right) =$$

$$\left(\frac{1}{\pi R^2}\right)^k \int_{A_1}\int_{A_2\setminus B_{x_1}}\int_{A_3\setminus B_{x_1}\bigcup B_{x_2}} ... \int_{A_k\setminus(\bigcup_{j=1}^{k-1} B_{x_j})} \prod_{j=1}^{k}\nu\left(B\setminus\bigcup_{v=j}^{k-1}B_{x_v}\right)^{i_j-i_{j-1}-1} dx_k...dx_1 \quad (3)$$

For $k = 1$, we get

$$\mathbb{P}\left(X_{i_1} \in A_1 | X_1 \in \Phi_M(n)\right) = \frac{1}{\pi R^2}\int_{A_1}\left(\frac{\nu\left(B\setminus B_{x_1}\right)}{\pi R^2}\right)^{i_1-1} dx_1 \quad (4)$$

Proof. The proof of equation 3 in the Proposition above is straightforward. We observe that the event $\{X_{i_j} \in A_j, \forall j \in \{1,..,k\}, X_{i_j} \in \Phi_M(n) \forall j \in \{1,..,k\}\}$ is verified if and only if:

- $\forall j \in \{1,..,k\}, X_{i_j}$ is located in $A_j \setminus \cup_{v=1}^{j-1} B_{X_v}$
- $\forall j \in \{1,..,k\}$, all the points with index bounded by $i_{j-1}+1$ and $i_j - 1$ do not lie in $\cup_{v=j}^{k} B_{X_v}$.

The first condition above ensures that all the points X_{i_j} are in A_j, and the second condition ensures that the points belong to $\Phi_M(n)$.

□

In the next Proposition, we compute the mean area covered by the union of balls B_{X_i}. Let $\Xi_M(n)$ be the random closed set defined as:

$$\Xi_M(n) \bigcup_{X_i\in\Phi_M(n)} B_{X_i}$$

We define the *packing density* as $\frac{\mathbb{E}[\Xi_M(n)]}{\pi R^2}$.

Proposition 2. *If $n \sim \lambda\pi R^2$ with $\lambda \in \mathbb{R}^+$, we get*

$$\begin{aligned}
\lim_{R\to+\infty} \frac{\mathbb{E}\left[\Xi_M(n)\right]}{\pi R^2} &= (1-e^{-\lambda\pi r^2}) \\
&- \frac{1}{\pi r^2}\int_{B(O,2r))\setminus B_O} \nu(B_O\cap B_y)\left(\frac{1-e^{-\lambda\nu(B_O\cup B_y)}}{\nu(B_x\cup B_y)} - \frac{e^{-\lambda\pi r^2}-e^{-\lambda\nu(B_O\cap B_y)}}{\nu(B_O\cup B_y)-\pi r^2}\right) dy \\
&+ \int_{B(O,2r)\setminus B_O}\int_{((B_O\cap B_y)\oplus B_O)\setminus(B_O\cup B_y)} \frac{\nu(B_O\cap B_y\cap B_z)}{\pi r^2}\left[\frac{1-e^{-\lambda a_{Oyz}}}{a_{yz}a_{Oyz}}\right. \\
&+ \left.\left(-\frac{1}{a_{yz}}+\frac{1}{a_{yz}-\pi r^2}\right)\frac{e^{-\lambda a_{yz}}-e^{-\lambda a_{Oyz}}}{a_{Oyz}-a_{yz}} - \frac{e^{-\lambda\pi r^2}-e^{-\lambda a_{Oyz}}}{(a_{yz}-\pi r^2)(a_{Oyz}-\pi r^2)}\right] dzdy \\
&- K_4(\lambda,r)+K_5(\lambda,r) \qquad (5)
\end{aligned}$$

The addition $\oplus$ is the Minkowski-addition (see [24] page 5 for a definition). The two functions $K_4(\lambda,r)$ and $K_5(\lambda,r)$ are detailed in appendix 8.1.

The proof of this proposition can be found in appendix 8.1. Note that for the numerical evaluation, the two first quantities of equation 5 are sufficient to obtain very accurate estimation of the packing density. In Figure 2(b), we confront the packing densities obtained by simulation and by evaluation of equation 5 considering either the first term or the two first terms. It appears clearly that the two first terms give a very accurate estimation of the packing density. We also observe that when λ tends to infinity, the packing density converges to ≈ 0.78.

5 A new CSMA-CA model

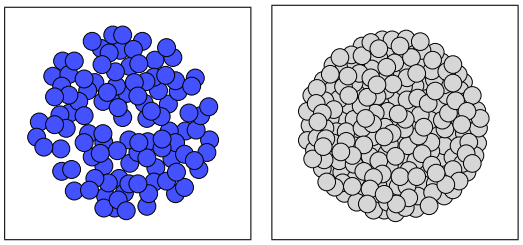

(a) A sample of a Matèrn point process.

(b) A sample of a SSI point process.

Figure 3: Samples of the Matèrn and SSI point process after saturation with $R = 1$ and $r = 0.1$.

As shown in Section 4, the Matèrn point process presents several flaws regarding the modeling of transmitters in a CSMA/CA network. In this section, we discuss another point process, the *Simple Sequential Inhibition* (SSI) point process, as being a valuable and more appropriate model for CSMA/CA networks. The SSI point process has been introduced by Palásti [19]. This model belong to a family of well-known models used in the context of *packing problems* or *space filling*. They are concerned with the distribution of *solids* in k-dimensional spaces [10, 23]. The SSI point process is also known as the Poisson disk distribution and is used in computer graphics to efficiently sample images [4, 27].

The SSI point process is a constructive point process distributed in a finite area of the plane, B in our case. Let $X_1, ..., X_n$ be a sequence of random variables independently and uniformly distributed in B. X_1 is systematically added to the SSI point process, denoted $\Phi_S(n)$. X_i is added to $\Phi_S(n)$ if $X_i \notin \cup_{X_j \in \Phi_S(i-1)} B_{X_j}$ where B_{X_j} is the ball centered in X_j with radius r. The process stops whenever the n points have been considered or when B is entirely covered by the union of the inhibition balls. As for the temporal Matèrn point process, this ball is an inhibition ball and only a subset of the initial n points are being finally selected.

We shall say that a sample of the SSI has reached saturation when the union of the inhibition balls of the selected points covers entirely B. Note that the temporal Matèrn point process is a thinning of the SSI. Interference generated by the points of the Matèrn point process is then a lower bound of the interference of the SSI point process. Figures 3(a) and 3(b) depict samples of Matèrn and SSI point processes after saturation. We can clearly see that with n large enough , the SSI covers entirely B whereas the Matèrn does not. The SSI model compensates for the main flaw of the Matèrn model as it considers only the effective transmitters inhibition balls during the selection process. Moreover, it offers a temporal scheduling equivalent to the temporal Matèrn one.

For the SSI process, very few theoretical results are existing. For instance, we have no result on the mean number of points in B or the probability for an initial point X_i to be selected. However, some values have been approximated. *E.g.*, the mean number of nodes in B after saturation can be approximated by $\frac{4c^2R^2}{r^2}$ where c is the *packing density* (in our case $c = 0.56$ [14]). It has been conjectured that the ratio $\frac{\mathbb{E}\left[\sum_{X_i \in \Phi_S}^{+\infty} \nu(B_i)\right]}{\pi R^2}$ converges to the constant $4c$. Other estimations approximate the distribution of nodes or the distance between closest points [12].

6 Interference with CSMA-CA protocols

In this Section we present a set of results on interference. We consider the level of interference at the center of the observation window B, denoted O. The temporal Matèrn process and the SSI process are both considered.

6.1 Mean and Variance of the interference for the modified Matèrn point process

From the distribution of a point in the Matèrn point process, we can easily deduce the mean interference level at O, according to the following Proposition.

Proposition 3.

$$\mathbb{E}\left[I_{\Phi_M(n)}(O)\right] = 2\pi \int_0^R u \frac{1 - \left(\frac{A(u,r,R)-\pi r^2}{\pi R^2}\right)^n}{\pi R^2 + \pi r^2 - A(u,r,R)} l(u) du$$

If n is constant and R tends to infinity, $\mathbb{E}[I_{\Phi_M(n)}(O)]$ tends to 0. If $n \sim \lambda \pi R^2$, we have

$$\lim_{R \to +\infty} \mathbb{E}\left[I_{\Phi_M(\lambda \pi R^2)}(O)\right] = \frac{1 - e^{-\lambda \pi r^2}}{\pi r^2} \int_{\mathbb{R}^2} l\left(\|x\|\right) dx$$

For the special attenuation function $l(u) = min(1, u^{-\alpha})$ with $\alpha > 2$, we have

$$\lim_{R\to+\infty} \mathbb{E}\left[I_{\Phi_M(\lambda\pi R^2)}(O)\right] = 2\frac{1-e^{-\lambda\pi r^2}}{r^2}\left(\frac{1}{2}+\frac{1}{\alpha-2}\right)$$

For the second moment:

$$\begin{aligned}\mathbb{E}\left[I^2_{\Phi_M(n)}(O)\right] &= \int_B \frac{1-\left(\frac{\nu(B\setminus B_x)}{\pi R^2}\right)^n}{\pi R^2-\nu(B\setminus B_x)} l\left(\|x\|\right)^2 dx \\ &+ 2\int_B\int_{B\setminus B_x} \frac{1}{\pi R^2-\nu(B\setminus B_x\cup B_y)}\Big[\frac{1-\left(\frac{\nu(B\setminus B_x\cup B_y)}{\pi R^2}\right)^{n-1}}{\pi R^2-\nu(B\setminus B_x\cup B_y)} \\ &- \frac{\left(\frac{\nu(B\setminus B_y)}{\pi R^2}\right)^{n-1}-\left(\frac{\nu(B\setminus B_x\cup B_y)}{\pi R^2}\right)^{n-1}}{\pi R^2\left(1-\frac{\nu(B\setminus B_x\cup B_y)}{\nu(B\setminus B_y)}\right)}\Big] dydx \qquad (6)\end{aligned}$$

When $R \to +\infty$ and $n \sim \lambda\pi R^2$,

$$\begin{aligned}\lim_{R\to+\infty} \mathbb{E}\left[I^2_{\Phi_M(n)}(O)\right] &= \frac{1-e^{-\lambda\pi R^2}}{\pi r^2}\int_{\mathbb{R}^2} l\left(\|x\|\right)^2 dx \\ &+ \frac{2}{\pi r^2}\int_{\mathbb{R}^2}\int_{\mathbb{R}^2\setminus B_x}\left[\frac{1-e^{-\lambda\nu(B_x\cup B_y)}}{\nu(B_x\cup B_y)}-\frac{e^{-\lambda\pi r^2}-e^{-\lambda\nu(B_x\cup B_y)}}{\nu(B_x\cup B_y)-\pi r^2}\right] \qquad (7) \\ &\quad l\left(\|x\|\right) l\left(\|y\|\right) dydx \qquad (8)\end{aligned}$$

The proof is presented in Appendix 8.2.

6.2 Mean and Variance of the interference for the SSI point process

There is no theoretical result about the distribution of $\Phi_S(n)$. However, the distribution of one point from $\Phi_S(n)$ can be approximated by the uniform distribution. Simulations have shown that for R large enough, the uniform distribution fits perfectly well with the distribution of one point arbitrarily chosen among the points of $\Phi_S(n)$. For smaller R (for instance $R = 1.0$ and $r = 0.1$), we observe some edge effects at the boundary of B. Under this assumption, we can derive the mean interference level:

$$\begin{aligned}\mathbb{E}\left[I_{\Phi_S(n)}(O)\right] &= \sum_{i=1}^{n}\mathbb{E}\left[l(\|X_i\|)\mathbb{1}_{X_i\in\Phi_S(n)}\right] \\ &\approx \mathbb{E}\left[N_S(n)\right]\frac{2}{R^2}\int_0^R ul(u)du\end{aligned}$$

where $N_S(n)$ is the number of points in $\Phi_S(n)$. Unfortunately, $\mathbb{E}[N_S(n)]$ is not known. Nevertheless, when the process has reached saturation ($n = +\infty$), it can be approximated by $\mathbb{E}[N_S(n)] \approx 4c\frac{R^2}{r^2}$ [14].

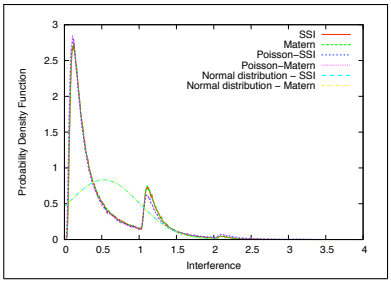

(a) Interference Probability Density Function. $R = 20.0$, $r = 1.0$, $n = 0.2\frac{R^2}{r^2}$, $S_i = 1$, $\alpha = 3$.

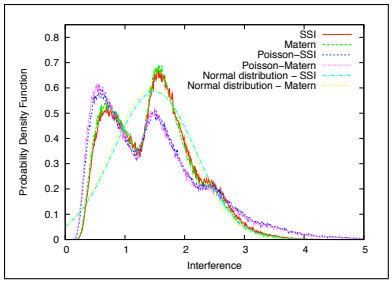

(b) Interference Probability Density Function. $R = 20.0$, $r = 1.0$, $n = 0.7\frac{R^2}{r^2}$, $S_i = 1$, $\alpha = 3$.

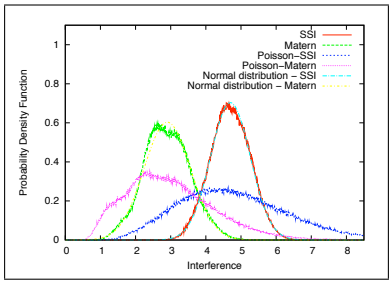

(c) Interference Probability Density Function. $R = 20.0$, $r = 1.0$, $n = 20.0\frac{R^2}{r^2}$, $S_i = 1$, $\alpha = 3$.

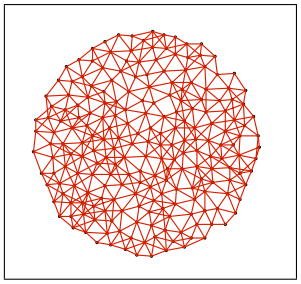

(d) Graph of SSI points after saturation ($n = +\infty$).

Figure 4: Interference PDF.

6.3 Convergence towards a Normal law

The interference PDF is unknown for both the SSI and the Matèrn point processes. Thus, in this Section, they are studied by simulation. In Figures 4(a), 4(b) and 4(c), we plot the interference PDF for the SSI and the Matèrn point processes. We also show two Gaussian distributions with mean and variance values equal to the ones of the SSI and Matèrn interference distributions. Finally, in order to compare the Matèrn and SSI interference distributions to the one generated by a Poisson point process, we have generated samples of two Poisson point processes in B with the same mean number of points as the Matèrn and SSI processes. The resulting interference PDF are denoted *Poisson Matèrn* and *Poisson SSI*.

Figure 4(a), correspond to a network with parameters $R = 2.0$, $r = 0.1$ and $n = 0.2\frac{R^2}{r^2}$. In such a sparse network, it appears that the interference generated by the Poisson point processes fit very well the SSI and Matèrn ones, contrarily to the Gaussian interference. Note that the two peaks in the PDF are due to the particular path-loss function that we have considered. For a non-sparse but non-dense network, $n = 0.7\frac{R^2}{r^2}$ in Figure 4(b), it appears that neither the Poisson interference distribution nor the Gaussian distribution fit the Matèrn and SSI interference.

Finally, while the network becomes saturated, $n = 20.0\frac{R^2}{r^2}$ in Figure 4(c), the interference generated by the SSI and Matèrn point processes seem to converge towards a Gaussian distribution. Given this observation, a χ^2 test with 0.05 significance level has been used to validate the hypothesis of a Normal distribution for the two point processes. The test has lead to the acceptation of the Normal distribution in both SSI and Matèrn cases.

Note that the use of a Poisson point process to model transmitters of a CMSA/CA network is only valid if the network is very sparse. In consequence, the method in [18] which proposes to considering a Poisson point process with an intensity equals to the Matèrn intensity is not adapted except in particular conditions.

The convergence of the SSI interference distribution towards a Gaussian one is a conjecture that we have only validated with a statistical test. If it happens to be exact, it would lead to a very interesting result on interference modeling for CSMA/CA networks. One hint about this convergence is the very regular structure induced by the transmitters location in the SSI model. After saturation, the number of points in each subset of B is almost surely bounded. The lower and upper bound are quite close to each other. The exclusion effect combined to the constraint on the coverage of B leads to very regular patterns. As an illustration, Figure 4(d) shows a graph where SSI points are connected if their distance is less than $2 * r$,. In other words, two points are neighbors if their inhibition balls overlap. As we can see, points in B seem quite regularly located. This pseudo-regularity has already been exploited in the context of computer graphics where several works [21, 4] proposed to use jittering of regular patterns, such as a regular grid, to approximate Poisson disk distributions, *i.e.* SSI distributions.

7 Conclusion and perspectives

In this article, we have discoursed about the modeling of interference for multi-hop wireless networks. We have presented the main limitations of the Poisson and Matèrn point processes classically used to model transmitters' location in wireless networks. If the Poisson model is adapted to non-CSMA/CA networks, it reveals to be inaccurate

in the context of CSMA/CA networks as it does not consider any dependancy between the different transmitters' location. The result is an inappropriate interference distribution except for sparse networks. The Matèrn point process leads to a more realistic model but still suffers from unexpected properties such as an underestimation of concomitant active transmitters and interference. In consequence, we have proposed the use of an alternate point process, the SSI one, which we assert being a valuable and more appropriate model for CSMA/CA networks. Moreover, we have conjectured that the interference distributions of the Matèrn and SSI models converge towards a Normal distribution contrarily to the Poisson model. This conjecture, not yet analytically proven, is very promising as it would provide the opportunity to analytically study and characterize values such as the Signal over Interference and Noise Ratio (SINR) or the Symbol Error Outage (SEO)...

There are two clear perspectives to the work presented in this article. The first one consists in proving the convergence of the Matèrn and SSI models towards the Normal distribution. The second one is to extend the interference model to consider other CCA modes. In other words, the models should be extended to considering the global interference level and no more exclusion balls when selecting the effective transmitters. We have taken a first step in this perspective with the proposition of constructive point processes such as the SSI one and our Temporal Matèrn. More studies now remain to be done.

8 Appendix

8.1 Proof of Proposition 2

The area of $\Xi_M(n)$ can be written as follows:

$$\begin{aligned}
\mathbb{E}\left[\Xi_M(n)\right] &= \mathbb{E}\left[\sum_{i=1}^{n} \nu\left(B \cap B_{X_i}\right) \mathbb{1}_{X_i \in \Phi_M(n)}\right] + \mathbb{E}\left[\sum_{i,j=1;j>i}^{n} \nu\left(B \cap B_{X_i} \cap B_{X_j}\right) \mathbb{1}_{(X_i,X_j) \in \Phi_M(n)}\right] \\
&+ \mathbb{E}\left[\sum_{i,j,k=1;k>j>i}^{n} \nu\left(B \cap B_{X_i} \cap B_{X_j} \cap B_{X_k}\right) \mathbb{1}_{(X_i,X_j,X_k) \in \Phi_M(n)}\right] \\
&+ \mathbb{E}\left[\sum_{i,j,k,l=1;l>k>j>i}^{n} \nu\left(B \cap B_{X_i} \cap B_{X_j} \cap B_{X_k} \cap B_{X_l}\right) \mathbb{1}_{(X_i,X_j,X_k,X_l) \in \Phi_M(n)}\right] \\
&+ \mathbb{E}\left[\sum_{i,j,k,l,m=1;m>l>k>j>i}^{n} \nu\left(B \cap B_{X_i} \cap B_{X_j} \cap B_{X_k} \cap B_{X_l} \cap B_{X_m}\right) \mathbb{1}_{(X_i,X_j,X_k,X_l,X_m) \in \Phi_M(n)}\right]
\end{aligned}$$

It corresponds to the classical way to compute the area of the union of several balls. In our case, the number of intersections is finite. Indeed, if we consider a point of the plane, this points cannot be covered with a positive probability by more than five balls of radius r and given that the centers of the balls are distant of at least r from each

others. We compute now each term of the equality. We get for the first term:

$$\begin{aligned}\mathbb{E}\left[\sum_{i=1}^{n}\nu\left(B\cap B_{X_i}\right)\mathbb{1}_{X_i\in\Phi_M(n)}\right] &= \frac{1}{\pi R^2}\int_B\sum_{i=1}^{n}\nu\left(B\cap B_x\right)\left(\frac{\nu(B\setminus B_x)}{\pi R^2}\right)^{i-1}dx\\ &= \int_B\frac{1}{\pi R^2-\nu(B\setminus B_x)}\nu\left(B\cap B_x\right)\left(1-\left(\frac{\nu(B\setminus B_x)}{\pi R^2}\right)^{n}\right)dx\end{aligned}$$

Suppose that $n\sim\lambda\pi R^2$ and R tends to infinity, so we can take $\pi R^2-\nu(B\setminus B_x)=\nu(B_x)=\pi r^2$ and $\nu(B\cap B_x)=\pi r^2$. Moreover, $\lim_{R\to+\infty}\left(\frac{\nu(B\setminus B_x)}{\pi R^2}\right)^{\lambda\pi R^2}=e^{-\lambda\pi r^2}$.

The limit is then

$$\lim_{R\to+\infty}\frac{\mathbb{E}\left[\sum_{i=1}^{n}\nu\left(B\cap B_{X_i}\right)\mathbb{1}_{X_i\in\Phi_M(n)}\right]}{\pi R^2} = 1-e^{-\lambda\pi r^2}$$

For the second term, we get:

$$\begin{aligned}&\mathbb{E}\left[\sum_{i,j=1;j>i}^{n}\nu\left(B\cap\left(B_{X_i}\cap B_{X_j}\right)\right)\mathbb{1}_{(X_i,X_j)\in\Phi_M(n)}\right]\\ &= \frac{1}{(\pi R^2)^2}\int_B\int_{B\setminus B_x}\sum_{i=1}^{n-1}\sum_{j=i+1}^{n}\nu\left(B\cap B_x\cap B_y\right)\left(\frac{\nu(B\setminus(B_x\cup B_y))}{\pi R^2}\right)^{i-1}\left(\frac{\nu(B\setminus B_y)}{\pi R^2}\right)^{j-i-1}dydx\\ &= \int_B\int_{(B\cap B(x,2r))\setminus B_x}\frac{\nu(B\cap B_x\cap B_y)}{\pi R^2-\nu(B\setminus B_x)}\left(\frac{1-\left(\frac{\nu(B\setminus(B_x\cup B_y))}{\pi R^2}\right)^{n-1}}{\pi R^2-\nu(B\setminus(B_x\cup B_y))}\right.\\ &- \left.\frac{\left(\frac{\nu(B\setminus B_x)}{\pi R^2}\right)^{n-1}-\left(\frac{\nu(B\setminus(B_x\cup B_y))}{\pi R^2}\right)^{n-1}}{\pi R^2-\pi R^2\frac{\nu(B\setminus B_x\cup B_y)}{\nu(B\setminus B_x)}}\right)dydx\end{aligned}$$

When R increases, we can neglect the edge effect, and if $n\sim\lambda\pi R^2$, the second integral does not depends on the location of x we get

$$\begin{aligned}&\mathbb{E}\left[\sum_{i,j=1;j>i}^{n}\nu\left(B\cap\left(B_{X_i}\cap B_{X_j}\right)\right)\mathbb{1}_{(X_i,X_j)\in\Phi_M(n)}\right]\\ &\sim \pi R^2\int_{B(O,2r))\setminus B_O}\frac{\nu(B_O\cap B_y)}{\pi r^2}\left(\frac{1-\left(\frac{\pi R^2-\nu(B_O\cup B_y)}{\pi R^2}\right)^{n-1}}{\nu(B_x\cup B_y)}\right.\\ &- \left.\frac{\left(\frac{\pi R^2-\pi r^2}{\pi R^2}\right)^{n-1}-\left(\frac{\pi R^2-\nu(B_O\cup B_y)}{\pi R^2}\right)^{n-1}}{\pi R^2-\pi R^2\frac{\pi R^2-\nu(B_O\cup B_y)}{\pi R^2-\pi r^2}}\right)dy\end{aligned}$$

We get,

$$\begin{aligned}&\lim_{R\to+\infty}\frac{\mathbb{E}\left[\sum_{i,j=1;j>i}^{n}\nu\left(B\cap\left(B_{X_i}\cap B_{X_j}\right)\right)\mathbb{1}_{(X_i,X_j)\in\Phi_M(n)}\right]}{\pi R^2}\\ &= \frac{1}{\pi r^2}\int_{B(O,2r))\setminus B_O}\nu(B_O\cap B_y)\left(\frac{1-e^{-\lambda\nu(B_O\cup B_y)}}{\nu(B_O\cup B_y)}-\frac{e^{-\lambda\pi r^2}-e^{-\lambda\nu(B_O\cap B_y)}}{\nu(B_O\cup B_y)-\pi r^2}\right)dy\end{aligned}$$

In the rest of the proof, we use, for convenience, the following notations: $a_z = \nu(B_z)$, $a_{yz} = \nu(B_y \cup B_z)$, $a_{Oyz} = \nu(B_O \cup B_y \cup B_z)$, etc. The same arguments as for the limit above lead to:

$$\begin{aligned}
&\lim_{R\to+\infty} \frac{\mathbb{E}\left[\sum_{i,j,k=1;k>j>i}^{n} \nu\left(B \cap B_{X_i} \cap B_{X_j} \cap B_{X_k}\right) \mathbb{1}_{(X_i,X_j,X_k)\in\Phi_M(n)}\right]}{\pi R^2} \\
&= \int_{B(O,2r)\setminus B_O} \int_{((B_O\cap B_y)\oplus B_O)\setminus(B_O\cup B_y)} \frac{\nu(B_O\cap B_y\cap B_z)}{\pi r^2} \left[\frac{1-e^{-\lambda a_{Oyz}}}{a_{yz}a_{Oyz}}\right. \\
&+ \left.\left(-\frac{1}{a_{yz}} + \frac{1}{a_{yz}-\pi r^2}\right)\frac{e^{-\lambda a_{yz}} - e^{-\lambda a_{Oyz}}}{a_{Oyz}-a_{yz}} - \frac{e^{-\lambda\pi r^2} - e^{-\lambda a_{Oyz}}}{(a_{yz}-\pi r^2)(a_{Oyz}-\pi r^2)}\right] dzdy
\end{aligned}$$

where $\oplus$ is the Minkowski-addition (see [24] page 5 for a definition).
For the 4^{th} and 5^{th} quantities, we get:

$$\begin{aligned}
&\lim_{R\to+\infty} \frac{\mathbb{E}\left[\sum_{i,j,k,l=1;l>k>j>i}^{n} \nu\left(B \cap B_{X_i} \cap B_{X_j} \cap B_{X_k} \cap B_{X_l}\right) \mathbb{1}_{(X_i,X_j,X_k,X_l)\in\Phi_M(n)}\right]}{\pi R^2} \\
&= \int_{B(O,2r)\setminus B_O} \int_{((B_O\cap B_y)\oplus B_O)\setminus(B_O\cup B_y)} \int_{((B_O\cap B_y\cap B_z)\oplus B_O))\setminus(B_O\cup B_y\cup B_z)} \frac{\nu(B_O\cap B_y\cap B_z\cap B_v)}{\pi r^2} \\
&\quad\times\left[\frac{1}{a_{zv}a_{yzv}a_{Oyzv}} + \left(-\frac{1}{a_{zv}a_{yzv}a_{Oyzv}} - \frac{c_1}{a_{Oyzv}-a_{yzv}} - \frac{c_2}{a_{Oyzv}-a_{zv}} + \frac{c_3}{a_{Oyzv}-\pi r^2}\right)e^{-\lambda a_{Oyzv}}\right. \\
&+ \left.\frac{c_1}{a_{Oyzv}-a_{yzv}}e^{-\lambda a_{yzv}} + \frac{c_2}{a_{Oyzv}-a_{zv}}e^{-\lambda a_{zv}} - \frac{c_3}{a_{Oyzv}-\pi r^2}e^{-\lambda\pi r^2}\right] dvdzdy
\end{aligned}$$

with

$$\begin{aligned}
c_1 &= -\frac{1}{a_{zv}a_{yzv}} - c_2 + c_3 \\
c_2 &= \frac{\pi r^2}{(a_{zv}-\pi r^2)a_{zv}(a_{yzv}-a_{zv})} \\
c_3 &= \frac{1}{(a_{zv}-\pi r^2)(a_{yzv}-\pi r^2)}
\end{aligned}$$

$$\lim_{R\to+\infty} \frac{\mathbb{E}\left[\sum_{i,j,k,l,m=1;m>l>k>j>i}^{n} \nu\left(B\cap B_{X_i}\cap B_{X_j}\cap B_{X_k}\cap B_{X_l}\cap B_{X_m}\right)\mathbb{1}_{(X_i,X_j,X_k,X_l,X_m)\in\Phi_M(n)}\right]}{\pi R^2}$$

$$= \int_{B(O,2r)\setminus B_O}\int_{((B_O\cap B_y)\oplus B_O)\setminus(B_O\cup B_y)}$$
$$\int_{((B_O\cap B_y\cap B_z)\oplus B_O))\setminus(B_O\cup B_y\cup B_z)}\int_{((B_O\cap B_y\cap B_z\cap B_v)\oplus B_O))\setminus(B_O\cup B_y\cup B_z\cup B_v)}$$
$$\frac{\nu(B_O\cap B_y\cap B_z\cap B_v\cap B_u)}{\pi r^2}\left[\frac{1}{a_{vu}a_{zvu}a_{yzvu}a_{Oyzvu}}+\left(-\frac{1}{a_{vu}a_{zvu}a_{yzvu}a_{Oyzvu}}-\frac{c_0^{'}}{a_{Oyzvu}-a_{yzvu}}\right.\right.$$
$$-\frac{c_1^{'}}{(a_{Oyzvu}-a_{zvu})(a_{yzvu}-a_{zvu})}-\frac{c_2^{'}}{(a_{Oyzvu}-a_{vu})(a_{Oyzvu}-a_{vu})}+\left.\frac{c_3^{'}}{(a_{Oyzvu}-\pi r^2)(a_{Oyzvu}-\pi r^2)}\right)$$
$$\times\ e^{-\lambda a_{Oyzvu}}+\frac{c_0^{'}}{a_{Oyzvu}-a_{yzvu}}e^{-\lambda a_{yzvu}}+\frac{c_1^{'}}{(a_{Oyzvu}-a_{zvu})(a_{yzvu}-a_{zvu})}e^{-\lambda a_{zvu}}$$
$$+\ \frac{c_2^{'}}{(a_{yzvu}-a_{vu})(a_{Oyzvu}-a_{vu})}e^{-\lambda a_{vu}}-\frac{c_3^{'}}{(a_{Oyzvu}-\pi r^2)(a_{yzvu}-\pi r^2)}e^{-\lambda\pi r^2}\Bigg]dvdzdy$$

with

$$\begin{aligned}
c_0^{'} &= -\frac{1}{a_{vu}a_{zvu}a_{yzvu}}-\frac{c_1^{'}}{a_{yzvu}-a_{zvu}}-\frac{c_2^{'}}{a_{yzvu}-a_{vu}}+\frac{c_3^{'}}{a_{yzvu}-\pi r^2}\\
c_1^{'} &= -\frac{1}{a_{vu}a_{zvu}}+c_3^{'}-c_2^{'}\\
c_2^{'} &= \frac{\pi r^2}{(a_{vu}-\pi r^2)a_{vu}(a_{zvu}-a_{vu})}\\
c_3^{'} &= \frac{1}{(a_{vu}-\pi r^2)(a_{zvu}-\pi r^2)}
\end{aligned}$$

8.2 Proof of Proposition 3

The mean interference is given by:

$$\begin{aligned}
\mathbb{E}\left[I_{\Phi_M(n)}(O)\right] &= \mathbb{E}\left[\sum_{i=1}^{n} l(\|X_i\|)\mathbb{1}_{X_i\in\Phi_M(n)}\right]\\
&= \frac{1}{\pi R^2}\int_B\sum_{i=1}^{n}\left(\frac{\nu(B\setminus B_x)}{\pi R^2}\right)^{i-1} l(\|x\|)dx\\
&= \int_B\frac{1-\left(\frac{\nu(B\setminus B_x)}{\pi R^2}\right)^n}{\pi R^2-\nu(B\setminus B_x)}l\left(\|x\|\right)dx\\
&= 2\pi\int_0^R u\frac{1-\left(\frac{A(u,r,R)-\pi r^2}{\pi R^2}\right)^n}{\pi R^2+\pi r^2-A(u,r,R)}l(u)du
\end{aligned}$$

If n is constant and R tends to infinity, $\mathbb{E}[I_{\Phi_M(n)}(O)]$ tends to 0. If $n\sim\lambda\pi R^2$, we get $\left(\frac{\nu(B\setminus B_x)}{\pi R^2}\right)^{\lambda\pi R^2}\to e^{-\lambda\pi r^2}$ and we can neglect the edge effects: $\pi R^2-\nu(B\setminus B_x)=\nu(B_x)=\pi r^2$.

We obtain:

$$\lim_{R\to+\infty} \mathbb{E}\left[I_{\Phi_M(\lambda\pi R^2)}(O)\right] = \frac{1-e^{-\lambda\pi r^2}}{\pi r^2}\int_{\mathbb{R}^2} l\left(\|x\|\right)dx$$

For the special attenuation function $l(u) = min(1, u^{-\alpha})$ with $\alpha > 2$, we get

$$\lim_{R\to+\infty} \mathbb{E}\left[I_{\Phi_M(\lambda\pi R^2)}(O)\right] = 2\frac{1-e^{-\lambda\pi r^2}}{r^2}\left(\frac{1}{2}+\frac{1}{\alpha-2}\right)$$

The second moment can also be obtained in the same way. By definition of the interference, we get:

$$\mathbb{E}\left[I^2_{\Phi_M(n)}(O)\right] = \mathbb{E}\left[\sum_{i=1}^{n} l\left(\|X_i\|\right)^2 \mathbb{1}_{X_i\in\Phi_M(n)}\right]$$

$$+2\mathbb{E}\left[\sum_{i=1}^{n-1}\sum_{j=i+1}^{n} l\left(\|X_i\|\right) l\left(\|X_j\|\right) \mathbb{1}_{X_i\in\Phi_M(n)}\mathbb{1}_{X_j\in\Phi_M(n)}\right]$$

For the first term on the right hand side of the equality, the computation is the same as the mean, we get

$$\mathbb{E}\left[\sum_{i=1}^{n} l\left(\|X_i\|\right)^2 \mathbb{1}_{X_i\in\Phi_M(n)}\right] = \int_B \frac{1-\left(\frac{\nu(B\setminus B_x)}{\pi R^2}\right)^n}{\pi R^2-\nu(B\setminus B_x)} l\left(\|x\|\right)^2 dx \tag{9}$$

For the second term, we get

$$\begin{aligned}
&\mathbb{E}\left[\sum_{i=1}^{n-1}\sum_{j=i+1}^{n} l\left(\|X_i\|\right) l\left(\|X_j\|\right) \mathbb{1}_{X_i\in\Phi_M(n)}\mathbb{1}_{X_j\in\Phi_M(n)}\right] \\
&= \frac{1}{(\pi R^2)^2}\int_B\int_{B\setminus B_x}\sum_{i=1}^{n-1}\sum_{j=i+1}^{n}\left(\frac{\nu(B\setminus B_x\cup B_y)}{\pi R^2}\right)^{i-1}\left(\frac{\nu(B\setminus B_y)}{\pi R^2}\right)^{j-i-1} l(\|x\|)l(\|y\|)dydx \\
&= \int_B\int_{B\setminus B_x}\frac{1}{\pi R^2-\nu(B\setminus B_x\cup B_y)}\Big[\frac{1-\left(\frac{\nu(B\setminus B_x\cup B_y)}{\pi R^2}\right)^{n-1}}{\pi R^2-\nu(B\setminus B_x\cup B_y)} \\
&\quad -\frac{\left(\frac{\nu(B\setminus B_y)}{\pi R^2}\right)^{n-1}-\left(\frac{\nu(B\setminus B_x\cup B_y)}{\pi R^2}\right)^{n-1}}{\pi R^2\left(1-\frac{\nu(B\setminus B_x\cup B_y)}{\nu(B\setminus B_y)}\right)}\Big] l(\|x\|)l(\|y\|)dydx
\end{aligned} \tag{10}$$

When $R\to+\infty$ and $n\sim\lambda\pi R^2$, we can neglect the edge effects, thus consider that $\pi R^2-\nu(B\setminus B_x\cup B_y) = \nu(B_x\cup B_y)$ and $\pi R^2 - \pi R^2\frac{\nu(B\setminus B_x\cup B_y)}{\nu(B\setminus B_y)} = \nu(B_x\cup B_y)-\nu(B_y) = \nu(B_x\cup B_y)-\pi r^2$.

Moreover,

$$\lim_{R\to+\infty}\left(\frac{\nu(B\setminus B_y)}{\pi R^2}\right)^{\lambda\pi R^2-1} = e^{-\lambda\pi r^2} \text{ and } \lim_{R\to+\infty}\left(\frac{\nu(B\setminus B_x\cup B_y)}{\pi R^2}\right)^{\lambda\pi R^2} = e^{-\lambda\nu(B_x\cup B_y)}$$

So, if R tends to infinity and $n\sim\lambda\pi R^2$, equations 9 and 10 lead to

$$\lim_{R\to+\infty} \mathbb{E}\left[I^2_{\Phi_M(n)}(O)\right] = \frac{1-e^{-\lambda\pi R^2}}{\pi r^2}\int_{\mathbb{R}^2} l\left(\|x\|\right)^2 dx$$

$$+\frac{2}{\pi r^2}\int_{\mathbb{R}^2}\int_{\mathbb{R}^2\setminus B_x}\left[\frac{1-e^{-\lambda\nu(B_x\cup B_y)}}{\nu(B_x\cup B_y)} - \frac{e^{-\lambda\pi r^2}-e^{-\lambda\nu(B_x\cup B_y)}}{\nu(B_x\cup B_y)-\pi r^2}\right] l\left(\|x\|\right) l\left(\|y\|\right) dydx$$

References

[1] F. Baccelli and B. Blaszczyszyn. On a coverage process ranging from the boolean model to the poisson voronoi tessellation, with applications to wireless communications. *Advances in Applied Probability*, 33:293–323, 2001.

[2] F. Baccelli, B. Błaszczyszyn, and P. Mühlethaler. An aloha protocol for multihop mobile wireless networks. *IEEE Transactions on Information Theory*, 52(2):421–436, 2006.

[3] C. Bettstetter, C. Hartmann, and C. Moser. How does randomized beamforming improve the connectivity of ad hoc networks. In *International Conference on Communications (ICC)*, pages 3380–85, Seoul, Korea, May 2005. IEEE.

[4] R. Cook. Stochastic sampling in computer graphics. *ACM Transactions on Graphics*, 5(1):51–72, 1986.

[5] O. Dousse, F. Baccelli, and P. Thiran. Impact of interferences on connectivity in ad hoc networks. *IEEE/ACM Transactions on Networking*, 13(2):425–436, April 2005.

[6] M. Franceschetti, O. Dousse, D. Tse, and P. Thiran. Closing the gap in the capacity of wireless networks via percolation theory. *IEEE Transactions on Information Theory*, 53(3):1009–1018, 2007.

[7] A. Ganesh and G. Torrisi. Large deviations of the interference in a wireless communication model. In *Modeling and Optimization in Mobile, Ad Hoc, and Wireless Networks (WiOpt)*, Limassol, Cyprus,, April 2007.

[8] P. Gupta and P. Kumar. *Critical Power for Asymptotic Connectivity in Wireless Networks*, pages 547–566. (Eds.) Birkhuser, Boston, USA, 1998.

[9] P. Gupta and P. Kumar. Capacity of wireless networks. *IEEE Transactions on Information Theory*, 46(2):388–404, 2000.

[10] P. Hall. *Introduction To the Theory of Coverage Processes*. Wiley, 1988.

[11] R. Hekmat and P. Van Mieghem. Study of connectivity in wireless ad-hoc networks with an improved radio model. In *Modeling and Optimization in Mobile, Ad Hoc, and Wireless Networks (WiOpt)*, Cambridge, UK, 2004.

[12] R. Herczynski. Distribution function for random distribution of spheres. *Nature*, 255:540–541, 1975.

[13] J. Ilow and D. Hatzinakos. Analytic alpha-stable noise modeling in a poisson field of interferers or scatterers. *IEEE Transactions on Signal Processing*, 46(6):1601–1611, June 1998.

[14] W. S. Jodrey and G. M. Tory. Random sequential packing in $I\!R^n$. *Journal of statistical computation and simulation*, 10:87–93, 1980.

[15] B. Matern. Meddelanden fran statens. *Skogsforskningsinstitut*, 2:1–144, 1960.

[16] D. Miorandi. The impact of channel randomness on coverage and connectivity of ad hoc and sensor networks. *IEEE Transactions on Wireless Communications*, 7(3):1062–1072, March 2008.

[17] D. Miorandi and E. Altman. Coverage and connectivity of ad-hoc networks in presence of channel randomness. In *Conference on Computer Communications (INFOCOM)*, volume 1, pages 491–502, Miami, USA, March 2005. IEEE.

[18] H.Q. Nguyen, F. Baccelli, and D. Kofman. A stochastic geometry analysis of dense ieee 802.11 networks. In *Conference on Computer Communications (INFOCOM)*, Anchorage, USA, May 2007. IEEE.

[19] I. Palasti. On some random space filling problem. *Publications of Mathematical Institute of Hungarian Academy of Sciences*, 5(1):353–359, 1960.

[20] S. Saunders. *Antennas and propagation for wireless communication systems*. Wiley, 1999.

[21] H. Shapiro and R. Silverman. Alias-free sampling of random noise. *SIAM Journal on Applied Mathematics*, 8(2):225–248, 1960.

[22] R. Sollacher, M. Greiner, and I. Glauche. Impact of interference on the wireless ad-hoc networks capacity and topology. *Wireless Networks*, 12(1):53–61, february 2006.

[23] H. Solomon and H. Weiner. A review of the packing problem. *Communications in Statistics and Theoretical Methods*, 15:2571–2607, 1986.

[24] D. Stoyan, W. Kendall, and J. Mecke. *Stochastic Geometry and Its Applications, 2nd Edition*. John Wiley and Sons Ltd, Chichester, UK, 1996.

[25] D. Tse and P. Viswanath. *Fundamentals of wireless communication*. Cambridge University Press, 2005.

[26] X. Yang and A. P. Petropulu. Co-channel interference modeling and analysis in a poisson field of interferers in wireless communications. *IEEE Transactions on Signal Processing*, 51(1):64–76, January 2003.

[27] J. Yellot. Spectral consequences of photoreceptor sampling in the rhesus retina. *Science*, 221:382–385, 1983.

Centre de recherche INRIA Grenoble – Rhône-Alpes
655, avenue de l'Europe - 38334 Montbonnot Saint-Ismier (France)

Centre de recherche INRIA Bordeaux – Sud Ouest : Domaine Universitaire - 351, cours de la Libération - 33405 Talence Cedex
Centre de recherche INRIA Lille – Nord Europe : Parc Scientifique de la Haute Borne - 40, avenue Halley - 59650 Villeneuve d'Ascq
Centre de recherche INRIA Nancy – Grand Est : LORIA, Technopôle de Nancy-Brabois - Campus scientifique
615, rue du Jardin Botanique - BP 101 - 54602 Villers-lès-Nancy Cedex
Centre de recherche INRIA Paris – Rocquencourt : Domaine de Voluceau - Rocquencourt - BP 105 - 78153 Le Chesnay Cedex
Centre de recherche INRIA Rennes – Bretagne Atlantique : IRISA, Campus universitaire de Beaulieu - 35042 Rennes Cedex
Centre de recherche INRIA Saclay – Île-de-France : Parc Orsay Université - ZAC des Vignes : 4, rue Jacques Monod - 91893 Orsay Cedex
Centre de recherche INRIA Sophia Antipolis – Méditerranée : 2004, route des Lucioles - BP 93 - 06902 Sophia Antipolis Cedex

Éditeur
INRIA - Domaine de Voluceau - Rocquencourt, BP 105 - 78153 Le Chesnay Cedex (France)
http://www.inria.fr
ISSN 0249-6399